Journal of Marine Science and Technology, Vol. 20, No. 6, pp. 618-623 (2012)
DOI: 10.6119/JMST-012-0328-2

ASSESSMENT OF DISASTER LOSSES IN RICE PADDY FIELD AND YIELD AFTER TSUNAMI INDUCED BY THE 2011 GREAT EAST JAPAN EARTHQUAKE

Yuei-An Liou[1], Hsueh-Chun Sha[1], Ting-Ming Chen[2], Tai-Sheng Wang[1], Yi-Ting Li[2], Yen-Cheng Lai[2], Min-Hsin Chiang[2], and Li-Teh Lu[3]

Key words: MODIS, rice field, rice yield, RICE algorithm.

ABSTRACT

The Great East Japan Earthquake on 11 March 2011 triggered an extremely destructive tsunami that hit the Tohoku region of Japan severely. According to data from the Ministry of Agriculture, Forestry, and Fishes of Japan, Tohoku accounted for 27.59% of Japan's rice yield in 2010. It is an impact to a country that relies on rice as its main food source. This paper utilizes remote sensing techniques to estimate the disaster losses in rice field and yield in Fukushima and Miyagi, the most severely damaged coastal prefectures of the Tohoku region, by using a developed Rice field Identification and riCe yield Estimate (RICE) algorithm for analyzing the satellite images. In this study, the pre- and post-earthquake MODIS/Terra satellite images are utilized. It is found the disaster losses in rice field are 1932.52 ha and 718.43 ha in Miyagi and Fukushima, respectively, which are expected to cause a decrease in annual rice yield by 9,472.60 tons in Miyagi and by 2,939.10 tons in Fukushima, equivalent to a total annual loss of $US 1411 Mio. Such loss will be, very unfortunately and undoubtfully enlarged by several orders of magnitude when the contamination of nuclear radiation on the surrounding environment is considered.

I. INTRODUCTION

A destructive earthquake hit northeastern Japan on March 11th 2011. It was one of the most devastating natural disasters over the past decades. The magnitude 9.0 earthquake unleashed a tsunami to overwhelm large areas of Tohoku Pacific coastal prefectures that produce more than one quarter of total rice yields in Japan [20]. For Asians, rice is the most important staple food, especially in Japan. Within the Asian monsoon climate zone, Japanese agriculture is characterized by rice production and high productivity allowing Japan's self sufficiency and support for the development of its society and economy [23]. For Japanese, rice plays a significant role because it shapes the diet, history, economy, and culture of the country. Rice is an integral part of Japan [28]. It is a symbol of spirit and the national crop [22]. Tohoku region's environment is ideal for agriculture and rice is one of the important industrial crops. However, this natural predominance has been threatened by the salinization and contamination of the terrains due to the influence of the tsunami and nuclear radiation. The resulting fertility loss will cause long-term impacts to local farmers and region's economy for many generations. It is thus worthwhile to investigate the disaster loss in rice field and yield due to The Great East Japan Earthquake and its chain-reaction events, tsunami and nuclear radiation leakage.

With the advantage of assessing environmental change over a large area, remotely sensed imageries have been extensively used to acquire a wide variety of information of the Earth's surface, ranging from military applications to environmental change detection in vegetation cover, water-pollution, and polar ice fluctuations [1, 3, 4, 6, 16, 26, 29]. Montzka *et al*. [21] indicated that as the land-use are found to have a large effect on a pollution, multispectral remotely sensed data are used to enhance the knowledge of land-use types. The advantages of using multispectral remotely sensed data instead of CORINE Land Cover for the modelling of nitrate concentrations in the leachate of the Rur catchment are presented and discussed in the paper.

Although the present technology and knowledge are still

Paper submitted 12/06/11; revised 03/09/12; accepted 03/28/12. Author for correspondence: Yuei-An Liou (e-mail: yueian@csrsr.ncu.edu.tw).
[1] *Center for Space and Remote Sensing Research, National Central University, Jhongli, Taiwan, R.O.C.*
[2] *Graduate Institute of Hakka Politics and Economics, National Central University, Jhongli, Taiwan, R.O.C.*
[3] *Center for General Education, National Central University, Jhongli, Taiwan, R.O.C.*

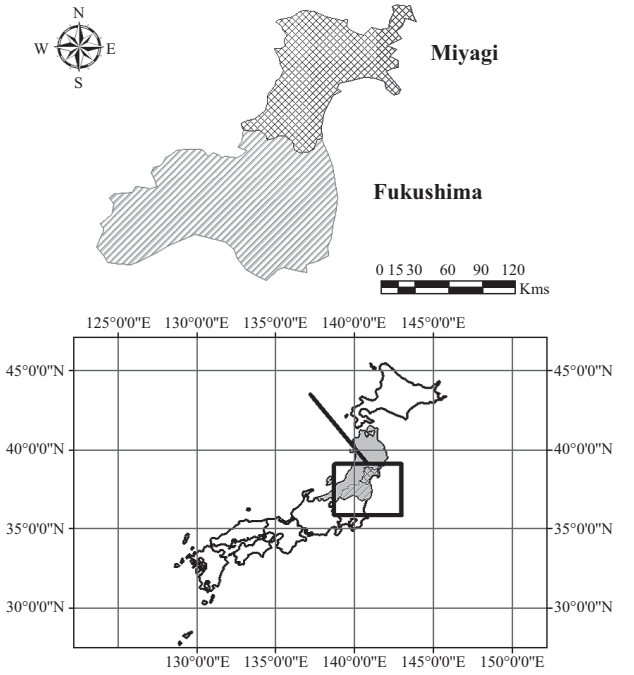

Fig. 1. Geographic Location of study area.

limited to prevent natural disasters, avoidance or mitigation of the disaster could be achieved with effective disaster management strategies along with proper utilization of remote sensing technology [17]. As the globe is facing more and more unpredictable natural disasters, geoinformatics resources management systems coordinated by GEO (Group on Earth Observations) and International Charter Space and Major Disasters serve as a crucial platform by providing prompt and rich information for hazard assessment, mitigation, and reduction after major natural disasters, such as May 5, 2008 Wenchuan earthquake in China, January 12, 2010 earthquake in Haiti, and March 11, 2011 Tohoku earthquake in Japan. The remote sensing technique that plays a vital role in the GEO platform is chosen to assess the disaster losses in rice field and yield caused by the Great East Japan Earthquake in this study.

From the literature, it is found that majority of the scientific reports in the field of remote sensing are concerned with mapping of the rice field or growth [5, 9, 11, 13, 14, 17, 25, 31]. In this study, it is our aim to present a newly developed Rice field Identification and riCe yield Estimate (RICE) algorithm for use with optical sensor data.

II. MATERIALS AND METHODS

1. Study Area

The Tohoku region is located in the northeastern portion of Honshu, the largest island of Japan (Fig. 1). It consists of six prefectures: Akita, Aomori, Yamagata, Iwate, Miyagi, and Fukushima. Tohoku is traditionally considered the granary of Japan because it supplies Sendai and the Tokyo-Yokohama

Table 1. 2010 Statistics of rice production.

Region	Miyagi	Fukushima	Tohoku	Japan
Rice area (ha)	73,400	80,600	419,300	1,625,000
Rice area (%)	4.52	4.96	25.80	100
Area (ha)	728,516	1,378,254	6,688,955	37,783,500
Area (%)	1.93	3.65	17.70	100
Rice yield (t)	400,000	445,700	2,339,000	8,478,000
Rice yield (%)	4.72	5.26	27.59	100

market with rice and other farm commodities (U.S. Library of Congress, http://countrystudies.us/japan/39.htm). The geographical size of the Tohoku region is 6.7 Mio ha, accounting for 17.7% of the total area in Japan as shown in Table 1. Nevertheless the rice field of the Tohoku region in 2010 was 0.42 Mio ha, accounting for 25.80% of total rice field in Japan.

Six prefectures of Tohoku region produced 2.3 Mio tons of rice in 2010, accounting for 27.59% of total rice yield in Japan. From the information above, it shows Tohoku region contributes a significant portion of the rice yield in Japan. Among the six prefectures, Miyagi and Fukushima that are the most damaged prefectures the Great East Japan Earthquake are chosen for this study. Note that Miyagi is the smallest one in the six prefectures, only accounting for 0.73 Mio ha (1.93% in Japan). However, according to report published by Japan MAFF (Ministry of Agriculture, Forestry, and Fishes), Miyagi produced 0.4 Mio tons of paddy rice in 2010 (4.72% in Japan) [20].

2. Data and Methodology

The MODIS Land Science Team provides a suite of standard MODIS data products to users, such as the MODIS Surface Reflectance 8-Day L3 Global 250 m (MOD09Q1) and 500 m (MOD09A1). The 7 of the 36 bands are designed for the study of vegetation and land surfaces, including blue (459-479 nm), green (545-565 nm), red (620-670 nm), near infrared (NIR1: 841-875 nm, NIR2: 1,230-1,250 nm), and shortwave infrared (SWIR1: 1,628-1,652 nm, SWIR2: 2,105-2,155 nm) [15].

The standard MODIS products are organized in a tile system with the sinusoidal projection. We obtained the 23 tiles (composites) including Jan., Apr., May, June, July, Nov., and Dec. of MODIS Surface Reflectance 8-Day L3 Global 250 m (MOD09Q1) and 500 m (MOD09A1) imageries for 2010 from NASA LP DAAC (http://lpdaac.usgs.gov/) to calculate vegetation indices, including Normalized Difference Vegetation Index (NDVI) [10], Enhanced Vegetation Index (EVI) [10], Land Surface Water Index (LSWI) [8], Normalized Difference Building Index (NDBI) [32], and Normalized Difference Snow Index (NDSI) [19] (Eqs. (1)-(5)) for discrimination between paddy fields and other land use type. Pixels containing snow at any time during the year were

Table 2. Parameters for each mask.

Parameters / Sutdy area	Forest mask	Cloud mask	Building mask	Rice equation	Sonw mask
Miyagi & Fukushima	NDVI ≧ 0.6 & LSWI > 0.1 or EVI > 0.45	Blue ref. ≧ 0.08	NDBI > 0	LSWI + 0.05 ≧ NDVI or LSWI + 0.05 ≧ EVI	NDSI > 0.4

excluded for the identification of paddy rice. The indices are shown as:

$$\mathrm{NDVI} = \frac{\rho_{NIR} - \rho_{red}}{\rho_{NIR} + \rho_{red}} \quad (1)$$

$$\mathrm{EVI} = 2.5 \times \frac{\rho_{NIR} - \rho_{red}}{\rho_{NIR} + 6 \times \rho_{red} - 7.5 \times \rho_{blue} + 1} \quad (2)$$

$$\mathrm{LSWI} = \frac{\rho_{NIR} - \rho_{SWIR}}{\rho_{NIR} + \rho_{SWIR}} \quad (3)$$

$$\mathrm{NDBI} = \frac{\rho_{SWIR} - \rho_{NIR}}{\rho_{SWIR} + \rho_{NIR}} \quad (4)$$

$$\mathrm{NDSI} = \frac{\rho_{GREEN} - \rho_{NIR}}{\rho_{GREEN} + \rho_{NIR}} \quad (5)$$

where ρ means reflectance, NIR is near infrared (841-845 nm), the wavelength of red band is 620-670 nm, blue band is 459-479 nm, and SWIR is shortwave infrared (1628-1652 nm).

The MODIS images were processed by the following steps: (1) mosaic images; (2) convert map projection from sinusoidal (SIN) to Geographic Lat/Lon & WGS84; (3) re-sampling the MOD09A1 (500 m resolution) to a spatial resolution of 250 m by nearest neighbor algorithm of ENVI software package; (4) combine the two bands of MOD09Q1 and 3-7 bands of MOD09A1 of the same date; and (5) locate the region of study area. These steps were adopted from the literature [9, 25, 31] with improved methodology and accuracy. In order to decrease the error of non-paddy rice discrimination the NDBI and NDSI were added to identify the Building and snow area. The MOD44W product was obtained from LP DAAC which was aimed to mask the water bodies. The DEM data at spatial resolutions of 90 m were obtained from the Shuttle Radar Topography Mission (http://srtm.csi.cgiar.org/) and used in the masking procedure associated with elevation criteria for identifying the rice field. The DEM map is also re-sampled as spatial resolutions of 250 m. An elevation of 150 m was chosen as a threshold of a land where it is unsuitable for rice planting. Note that the most suitable elevation threshold may certainly vary with geographic location. To optimize its choice, we thus conduct literature review and obtain the number 150 m as the threshold in our study [2, 27, 30, 31].

3. Algorithm for Identifying Rice Field

European and Asia rice is usually grown under flooded conditions ("paddy" rice) [7, 30]. Confalonieri *et al*. [7] indicated that modelling studies are important to investigate the relationship between crop management, productivity and environmental impact of paddy rice systems. Therefore, Confalonieri *et al*. and Xiao *et al*. used the different methods, Water Accounting Rice Model and temporal profile analysis of MODIS-derived indices, to identify the rice field, respectively.

During the rice flooding period, the LSWI values became higher than the vegetation indices (LSWI ≧ EVI or NDVI) [31]. According to the statistical data from Japan MAFF the flooding period of Fukushima and Miyagi is May [20]. Therefore, the relationship between LSWI and vegetation indices at the period of flooding was used to identify the rice field:

$$\mathrm{LSWI} + \underline{T} \geqq \mathrm{EVI} \text{ or } \mathrm{LSWI} + \underline{T} \geqq \mathrm{NDVI} \quad (6)$$

where T that can be varying and indeed depends on the local rice planting system, such as flooding/transplanting practices, and single, early, or late rice growth period. In this study, a global threshold (T) value of 0.05 recommended by Xiao *et al*. [31] is adopted. In order to accurately identify the rice field, the study conjecture that the elevation under 150 m was unsuitable for rice planting [31], and different masks were made for forest, evergreen vegetation, snow, building, and cloud (Table 2). To optimize the performance of these masking procedures, we found that satellite images of at least three months must be used to discriminate the characteristics of each land use type. The May images was used to identify paddy rice because the MAFF database shows the flooding and transplanting of the study is May; the January, May, and June images were used to identify forest; the January, November, and December images were used to identify snow; and all images (23 tiles) were used to identify building and cloud. Moreover, the results of identification of each non-paddy rice region and cloud were excluded. The spatial distribution of paddy rice was obtained through the RICE algorithm. The ground truth data of paddy rice spatial distribution could not be obtained easily, the reference data are generally based on high-resolution imagery in the earlier studies [12, 25, 31]. Therefore, we applied the high-resolution imagery of the Geo-eyes of Google Earth as the ground truth data. The scheme proposed by Xiao *et al*. [31] is aimed for the rice field identification, but not for the rice yield. The same algorithm is subsequently adopted by Peng *et al*. [25]. On the other hand,

Table 3. A comparison of rice field in study area between MODIS RICE algorithm and MAFF statistical data.

Statistics / Prefectures	2010 rice field from MAFF	Rice field estimation from MODIS data	Difference	Difference (%)
Miyagi (ha)	73,400	76,676	3,275	4.46
Fukushima (ha)	80,600	89,050	8,450	10.48
Miyagi (t)	400,000	412,066	12,066	3.01
Fukushima (t)	445,700	478,752	33,052	7.41

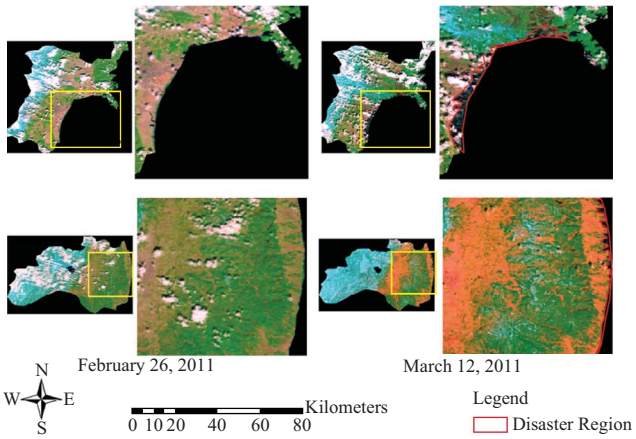

Fig. 2. MODIS images in study area after Tsunami (red region).

our newly developed algorithm, Rice field Identification and riCe yield Estimate (RICE) algorithm, is not only improved upon the rice identification scheme of Xiao *et al*. [31] with an embed semi-automatic function with higher computational efficiency and a NDBI for masking building to identify rice field, but also estimates the rice yield with the statistics regression concept.

4. Disaster Region Mapping

For precise estimates of the disaster loss in rice yield in Miyagi and Fukushima, through Editor tool of Geographic Information System (GIS). For mapping the disaster region in this study, the two images acquired on February 26, 2011 and March 12, 2011 are used, respectively. The pre- and post-earthquake MODIS multispectral images (250 m) are collected in Tohoku after tsunami from the MODIS Website (http://modis.gsfc.nasa.gov/). The land change is determined by the association with the type of the disaster [26]. For the case of this study, the land change type is focused on the inundation region due to impact of tsunami.

III. RESULTS AND DISCUSSIONS

1. Disaster regions in Miyagi and Fukushima

For mapping the disaster region in Tohoku after tsunami, pre- and post-earthquake MODIS multispectral images (250 m × 250 m) collected on 26 February and 12 March 2011 were used, respectively, as depicted in Fig. 2. It is observable

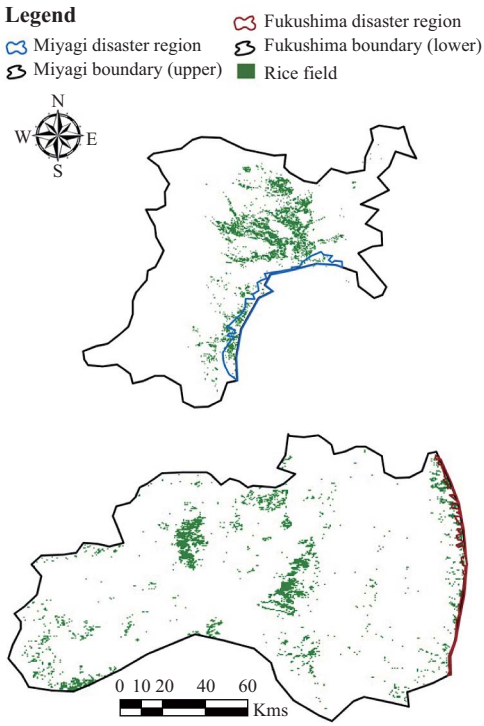

Fig. 3. Rice field derived from MODIS images.

that the inundated areas are located in the southeastern coastal regions of Miyagi and in the eastern coastal regions of Fukushima. It is visibly evident that the disaster losses in area are larger in Miyagi than Fukushima as reported in the mass communication.

2. Disaster Loss in Rice Field

In this study, the MODIS data were used to identify the rice field and subsequently the rice yield through a regression correlation. Fig. 3 shows the spatial distribution of the rice field in the two prefectures of interest in 2010. The number of pixels of rice field was converted to the rice planting area. The derived areas by the RICE algorithm are 76,675 and 89,050 ha in Miyagi and Fukushima, respectively. They were then compared with the ground truth data. The relative errors were satisfactory small, 4.46% for Miyagi and 10.48% for Fukushima as listed in Table 3. The errors are much smaller than those given in the literature by 5% or more as compared to the relative errors of 16.5% to 40% by Xiao *et al*. [31] and of 4% to 15.7% by Peng *et al*. [25]. The disaster losses in

Table 4. The loss of rice field in study area after 2010 tsunami.

Statistics / Prefectures	2010 total rice fields (MAFF) (ha)	Disaster loss of rice fields (MODIS) (ha)	Disaster loss of rice fields (MODIS) (%)	Disaster loss of rice yield (tons)	Disaster loss of rice yield (%)
Miyagi	73,400	1,932.52	2.63	9,472.60	2.37
Fukushima	80,600	718.43	0.89	2,939.10	0.66

rice field are subsequently calculated, 1,932.52 ha for Miyagi and 718.43 ha for Fukushima, accounting for 2.63% and 0.89% of the total rice planting areas of the two prefectures, respectively.

3. Disaster Loss in Rice Yield

Rice yield estimation relied on its regression correlation with the planting area. The regression correlation was determined by applying the 2001-2010 ground truth data of MAFF [20], but excluding the 2003 data. This is because the rice yield was significantly reduced in 2003, possibly due to two 7.0 and 8.0 scale earthquakes. The regression formula is determined as Yield = 5.3888xArea-1120.3, $R^2 = 0.99$. By utilizing the derived regression correlation, it is expected that the direct annual loss in rice yield will be 9,472.60 tons in Miyagi and 2,939.10 tons in Fukushima, accounting for 2.37% and 0.66% of their corresponding total rice yield (Table 4). The algorithms are different from some previous studies that had used Modeling approach with ground data to estimate crop yield [5, 24]. The *Rice field Identification and riCe yield Estimate* (RICE) algorithm could immediately obtain rice spatial distribution and yields from satellite imagery.

IV. CONCLUSIONS

By utilizing MODIS imagery, this paper assesses the disaster loss in rice field and yield in Miyagi and Fukushima, the most damaged prefectures during the 2011 Great East Japan Earthquake. The identification of rice field was performed by using a newly developed Rice field Identification and riCe yield Estimate (RICE) algorithm that was developed for remotely-sensed imagery. The performance of the RICE algorithm is very satisfactory with accuracy of area coverage better than those of the algorithms published in the literature by about 5% or more [18, 25, 27, 30, 31]. The disaster losses in rice field are found to be 1,932.52 ha for Miyagi and 718.43 ha for Fukushima. They will result in corresponding expected losses of rice yield by 9,472.60 tons and by 2,939.10 tons, respectively, in a year, equivalent to a direct total loss of $US 31 Mio in a year (based on an exchange rate of 1 USD *vs.* 80 JPY), assuming a market price of rice provided by MAFF. It is thus estimated that the direct economic loss in total agricultural products will be around $US 1411 Mio in a year since rice yield of Miyagi and Fukushima accounts for about 2.2% of the value of all kinds of agricultural products. Unfortunately, the arable field is submerged by salty ocean water due to tsunami and will be unsuitable for cultivation for another ten years at least. Nevertheless, the situation is even worse with the contamination of nuclear radiation. Besides, the problem of the nuclear radiation leakage of the Fukushima 1 Nuclear Power Plant is not resolved at the time of this study. Furthermore, it is inevitably that economic impact will regrettably persist for decades.

ACKNOWLEDGMENTS

We are grateful to the National Science Council (NSC) of Republic of China for financial support grant no. NSC-98-2111-M-008-012-MY3 and grant no. NSC 98-2410-H-008-044-MY2.

REFERENCES

1. Boyd, D. S., Foody, G. M., and Ripple, W. J., "Evaluation of approaches for forest cover estimation in the Pacific Northwest, USA, using remote sensing." *Applied Geography*, Vol. 22, pp. 375-392 (2002).
2. Bridhikitti, A. and Overcamp, T. J., "Estimation of Southeast Asian rice paddy areas with different ecosystems from moderate-resolution satellite imagery," *Agriculture, Ecosystems and Environment*, Vol. 146, pp. 113-120 (2012).
3. Chang, T.-Y., Liou, Y.-A., Lin, C.-Y., Liu, C.-S., and Wang, Y.-C., "Evaluation of surface heat fluxes in Chiayi plain of Taiwan by remotely sensed data," *International Journal Remote Sensing*, Vol. 31, No. 14, pp. 3885-3898, DOI: 10.1080/01431161.2010.483481 (2010).
4. Chang, T.-Y., Wang, Y. C., Feng, C.-C., Ziegler, A. D., Giambelluca, T. W., and Liou, Y.-A., "Estimation of root zone soil moisture using apparent thermal inertia with MODIS imagery over the tropical catchment of northern Thailand," *IEEE Journal of Selected Topics in Applied Earth Observations and Remote Sensing* (JSTARS), Vol. 5, pp. 752-761 (2012).
5. Chen, J., Lin, H., and Pei, Z., "Application of ENVISAT ASAR data in mapping rice crop growth in Southern China," *IEEE Geoscience Remote Sensing Letters*, Vol. 4, pp. 431-435 (2007).
6. Choe, E., Meer, F., Ruitenbeek, F., Werff, H., Smeth, B., and Kim, K. W., "Mapping of heavy metal pollution in stream sediments using combined geochemistry, field spectroscopy, and hyperspectral remote sensing: A case study of the Rodalquilar mining area," *Remote Sensing of Environment*, Vol. 112, pp. 3222-3233 (2008).
7. Confalonieri, R., Bellocchi, G., Tarantola, S., Acutis, M., Donatelli, M., and Genovese, G., "Sensitivity analysis of the rice model WARM in Europe: Exploring the effects of different locations, climates and methods of analysis on model sensitivity to crop parameters," *Environment Modelling & Software* Vol. 25, pp. 479-488 (2010).
8. Gao, B. C., "NDWI - a normalized difference water index for remote sensing of vegetation liquid water from space," *Remote Sensing of Environment*, Vol. 58, pp. 257-266 (1996).
9. Gao, J., Pan, G., Jiang, X., Pan, J., and Zhuang, D., "Land-use induced changes in topsoil organic carbon stock of paddy fields using MODIS and TM/ETM analysis: A case study of Wujiang County," *Journal of*

Environmental Sciences, Vol. 20, pp. 852-858 (2008).
10. Huete, A., Didan, K., Miura, T., Rodriguez, E. P., Gao, X., and Ferreira, L. G., "Overview of the radiometric and biophysical performance of the MODIS vegetation indices," *Remote Sensing of Environment*, Vol. 83, pp. 195-213 (2002).
11. Kurosu, T., Fujita, M., and Chiba, K., "Monitoring of rice crop growth from space using ERS-1 C-band SAR," *IEEE Transaction on Geoscience Remote Sensing*, Vol. 33, pp. 1092-1096 (1995).
12. Le Toan, T., Laur, H., Mougin, E., and Lopes, A., "Multitemporal and dualpolarization observations of agricultural vegetation covers by X-band SAR images," *IEEE Transaction on Geoscience Remote Sensing*, Vol. 27, pp. 709-718 (1989).
13. Le Toan, T., Ribbes, F., Wang, L.-F., Floury, N., Ding, K.-H., Kong, J. A., Fujita, M., and Kurosu, T., "Rice crop mapping and monitoring using ERS-1 data based on experiment and modeling results," *IEEE Transaction on Geoscience Remote Sensing*, Vol. 35, pp. 41-56 (1997).
14. Liew, S. C., Kam, S.-P., Tuong, T.-P., Chen, P. V., Minh, Q., and Lim, H., "Application of multitemporal ERS-2 synthetic aperture radar indelineating rice cropping systems in the Mekong River Delta, Vietnam," *IEEE Transaction on Geoscience Remote Sensing*, Vol. 36, pp. 1412-1420 (1998).
15. Lillesand, T. M., Kiefer, R. W., and Chipman, J. W., *Remote Sensing and Image Interpretation*, Wiley & Sons, New York, U.S.A., pp. 784 (2004).
16. Liou, Y.-A., Liu, S. F., and Wang, W. J., "Retrieving soil moisture from simulated brightness temperatures by a neural network" *IEEE Geoscience Remote Sensing Letters*, Vol. 39, pp. 1662-1673 (2001).
17. Liou, Y. A., Kar, S. K., and Chang, L. Y., "Use of high-resolution FORMASAT-2 satellite image for post-earthquake disaster assessment: a study following 12 May 2008 Wenchuan Earthquake," *International Journal of Remote Sensing* Vol. 31, No. 13, pp. 3355-3368, DOI: 10.1080/01431161003727655 (2010).
18. Liou, Y. A., Sha, H. C., Liao, L. W., and Chen, S. W., "Estimate of paddy rice yield in Chiayi plain of southern Taiwan based on MODIS data," *Cross-Strait Remote Sensing Workshop*, Chung-Li, Taiwan (2010).
19. Lopez, P., Sirguey, P., Arnaud, Y., Pouyaud, B., and Chevallier, P., "Snow cover monitoring in the Northern Patagonia Icefield using MODIS satellite images (2002-2006)," *Global and Planetary Change*, Vol. 61, pp. 103-116 (2008).
20. MAFF, The Ministry of Agriculture Forestry and Fisheries of Japan, Tokyo, Japan, Available online at: http://www.maff.go.jp/e/index.html (accessed 30 March, 2011).
21. Montzka, C., Canty, M., Kreins, P., Kunkel, R., Menz, G., Vereecken, H., and Wendland, E., "Multispectral remotely sensed data in modeling the annual variability of nitrate concentrations in the leachate," *Environment Modelling & Software*, Vol. 23, pp. 1070-1081 (2008).
22. Nakano, Y., Miyazaki, A., Yoshida, T., Ono, K., and Inoue, T., "A study on pesticide run off from paddy fields to a river in rural region," *Water Research*, Vol. 38, pp. 3017-3022 (2004).
23. Ogino, Y. and Ota, S., "The evolution of Japan's rice field drainage and development of technology," *International Science*, Vol. 56, pp. 69-80 (2007).
24. Pan, G., Sun, G. J., and Li, F. M., "Using QuickBird imagery and production efficiency model to improve crop yield estimation in the semiarid hilly Loess Plateau, China," *Environmental Modeling & Software*, Vol. 24, pp. 510-516 (2009).
25. Peng, D., Huete, A. R., Huang, J., Wang, F., and Sun, H., "Detection and estimation of mixed paddy rice cropping patterns with MODIS data," *International Journal of Applied Earth Observation and Geoinformation*, Vol. 13, pp. 13-23 (2011).
26. Piwowar, J. M., Pdeele, D. R., and Ledrew, E. F., "Temporal mixture analysis of Arctic sea ice imagery: a new approach for monitoring environmental change," *Remote sensing of Environment*, Vol. 63, pp. 195-207 (1998).
27. Sun, H. S., Huang, J. F., Huete, A. R., Peng, D. L., and Zhang, F., "Mapping paddy rice with multi-date moderate-resolution imaging spectroradiometer (MODIS) data in China," *Journal of Zhejiang University SCIENCE*, Vol. 10, pp. 1509-1522 (2009).
28. Takeo, K., "Japan's rich rice culture," *Japan Quarterly*, Vol. 46, pp. 58-63 (1999).
29. Wang, Y.-C., Chang, T.-Y., Liou, Y.-A., and Ziegler, A., "Terrain correction for increased estimation accuracy of evapotranspiration in a mountainous watershed," *IEEE Geoscience Remote Sensing Letters*, Vol. 7, No. 2, pp. 352-356, DOI: 10.1109/LGRS.2009.2035138 (2010).
30. Xiao, X. M., Boles, S., Frolking, S., Li, C., Babu, J. Y., Salas, W., and Mooer, B., "Mapping paddy rice agriculture in south southeast Asia using multi-temporal MODIS images," *Remote Sensing of Environment*, Vol. 100, pp. 95-113 (2006).
31. Xiao, X. M., Boles, S., Liu, J. Y., Zhuang, D. F., Frolking, S., Li, C. S., Salas, W., and Mooer, B., "Mapping paddy rice agriculture in southern China using multi-temporal MODIS images," *Remote Sensing of Environment*, Vol. 95, pp. 480-492 (2005).
32. Zha, Y., Gao, J., and Ni, S., "Use of normalized difference built-up index in automatically mapping urban areas from TM imagery," *International Journal of Remote Sensing*, Vol. 24, pp. 583-594 (2003).